https://doi.org/10.1038/s44383-025-00001-9

PDLP5, a plasmodesmata permeability regulator, can traffic between plant cells

Yumin Kan ✉ & Vitaly Citovsky

Plasmodesmata (PD) are membranous nanopores that connect the cytoplasm of neighboring plant cells and enable the cell-to-cell trafficking of nutrients and macromolecules, as well as invading viruses. PD plays a critical role in regulating intercellular communication, contributing to plant development, environmental responses, and interactions with viral pathogens. The PD proteome includes two major types of functional proteins, PD callose binding proteins (PDCBs) and PD-located proteins (PDLPs), involved in manipulating the size of PD pores. Most studies of PDCBs and PDLPs focused on their effects on the PD transport of different cargo molecules; yet, whether these PD proteins themselves have the capacity for cell-to-cell movement remains largely obscure. Here, we addressed this question by demonstrating that PDLP5, but not PDLP1 and PDLP2, can move efficiently from cell to cell in *Nicotiana benthamiana* and that this movement involves the native transmembrane domain of PDLP5. These observations would be useful for a better understanding of the complexity of the PDLP5 protein function during the processes of PD transport.

Plant intercellular connections, the plasmodesmata (PD), are specialized nanochannels that enable the trafficking of nutrients, and macromolecules—e.g., RNAs, proteins, hormones—as well as invading viruses between adjacent cells[1–3], and therefore play an essential role in regulating intercellular communication associated with plant growth, development, responses to the environment, and interactions with viral pathogens[4,5]. PD initially forms during cytokinesis, with a large number of PD inserted into the new cell walls between the two daughter cells, thus connecting the two cells and supplying the channels for cell-to-cell communication[1,6]. As membrane-rich structures, PDs contain the endoplasmic reticulum (ER)-derived membrane, a trans-PD desmotubule, in the central part of the pores that are lined by the plasma membrane[1,6]. Comparative proteomic approaches identified numerous PD proteins[7,8]; for example, recent plasmodesmata in silico proteome 1 (PIP1) bioinformatics tool predicted PD proteins in 22 plant species[9]. To date, the combination of the experimental and in silico approaches identified several major classes of PD functional proteins, which include β-1,3-glucanases (BGs), callose synthases (CALSs), callose-binding proteins (PDCBs), plasmodesmata-located proteins (PDLPs), multiple C2 domains transmembrane region proteins (MCTPs)[1], and leucine-rich repeat receptor-like kinases (RLK)[10]. PD channels are gateable, and they alter their permeability to allow the transport of macromolecules. PD gating is thought to be directly controlled by the formation or hydrolysis of callose (β-1,3-glucan) deposits at the neck regions of PD, resulting in their constriction or relaxation, respectively[11,12]. Interestingly, many pathogenic microbes, including fungi, bacteria, and viruses, can manipulate the PD permeability or structure during infection[5,13,14]; in fact, one of the first classes of macromolecules demonstrated to traffic through PD and increase PD permeability were the movement proteins (MPs) of plant viruses that mediate viral transmission between the host cells[5,15]. This manipulation of PD permeability and its control involve activities of different PD proteins, including PDLPs, which are conserved in higher plants and likely function as receptor-like kinases[16]. Specifically, in *Arabidopsis*, there are eight PDLPs, PDLP1-8[3]. Perhaps one of the most intriguing among them is PDLP5, a multifunctional protein that negatively regulates PD permeability and promotes plant innate immunity[4,17,18].

PDLP5 contains an N-terminal signal peptide followed by two copies of the conserved salt stress response/antifungal domain, also known as plant-specific cysteine-rich domain of unknown function 26 (DUF26), and a C-terminal transmembrane domain (TMD) with a very short cytoplasmic tail[4,19,20]. PDLP5 localizes to the central region of the PD channel and negatively regulates molecular transport through PD by stimulating callose deposition through activation of callose synthases (CalS) 1 and 8[4,19]. Consistent with this functionality, the PDLP5 loss- or gain-of-function mutants exhibit increased or decreased PD permeability, respectively[4,21], whereas destabilization of PDLP5, together with PDLP7, by the HopO1-1 effector protein of a phytopathogenic bacterium *Pseudomonas syringae* pv. *tomato* DC3000 enhances intercellular traffic in *Arabidopsis*[14]. Also, PDLP5, when expressed ectopically, induces the accumulation of salicylic acid and promotes innate immunity against pathogenic bacteria[18]. Unlike the non-redundant function of PDLP5, PDLP1, which is also involved in plant

Department of Biochemistry and Cell Biology, State University of New York, Stony Brook, NY, USA. ✉e-mail: yumin.kan@stonybrook.edu

immunity[22] and PD transport[3], shares functional redundancy with PDLP2 and PDLP3[3].

Collectively, these observations indicate that PDLP5 sorts into PD and regulates PD transport. But what is the fate of PDLP5 itself once it reaches PD? Here, we examined the idea that at least some PDLP5 molecules, having reached PD and exerted their activity in these channels, exit PD and translocate to adjacent cells. Our data indeed suggest that PDLP5 can move from cell to cell and this movement involves the native TMD of the protein. In contrast, two other members of the PDLP protein family, PDLP1 and PDLP2, as well as another cellular PD protein, PDCB1, did not exhibit the same capacity for intercellular transport. These results shed new and unexpected light on the complexity of the PDLP5 protein function during transport through PD.

Results

PDLP5 moves from cell to cell

We investigated whether PDLP5 located within PD, as schematized in Fig. 1a, can exit this channel and travel through it to the neighboring cells. To this end, PDLP5 was tagged at its C-terminus with the EGFP reporter and transiently expressed in *Nicotiana benthamiana* leaf tissues. Confocal microscopy analysis revealed two main patterns of PDLP5-EGFP accumulation in the leaf: single cells and multi-cell clusters in which the initially expressing cells exhibit higher signal intensity than their neighboring cells (Fig. 1b); in such patterns, protein accumulation in single cells indicates the lack of cell-to-cell movement and two- or three-cell clusters are diagnostic of protein transport through PD[23,24].

The cell-to-cell movement assay scores cells at relatively low magnification to allow visualization of the signal-containing cells and the surrounding areas of the tissues. Thus, we also examined these cells under high magnification to verify the localization of PDLP5 at PD. Figure 2 shows that PDLP5-EGFP accumulated in a characteristic peripheral punctate pattern diagnostic for PD[25–27]. Indeed, these PDLP5-EGFP puncta colocalized with the aniline blue staining pattern of the PD-associated callose deposits in the same cells (Fig. 2). In the positive control experiments, the *Turnip vein-clearing virus* (TVCV) MP, a known PD-associated viral protein[5,15], and PDCB1, a known PD-associated plant protein[28,29], accumulated in similar PD puncta that colocalized with the aniline blue staining. Furthermore, a significant fraction of PDCB1 also associated with ER, colocalizing with the SP-mRFP-KDEL ER marker (Fig. 2). Free EGFP, used as a negative control, showed no PD puncta, instead exhibiting its characteristic nucleocytoplasmic subcellular localization (Fig. 2b). Thus, although low magnification images detected some of PDLP5-EGFP in the cell cytoplasm (Fig. 1b), where the protein is synthesized, most of the signal accumulated in PD.

Next, we analyzed and quantified the ability of PDLP5 to move between cells by scoring the PDLP5-EGFP signal in multi-cell clusters. Figure 3a explores the optimal timing for the detection of the PDLP5-EGFP movement, demonstrating that whereas at 48 h post infiltration (hpi) only very low levels of the movement were detected, substantial and statistically significant movement was observed at later time points, i.e., 72 hpi and 120 hpi. Importantly, we detected no differences between the movement of these proteins at 48 hpi but, at 72 hpi and 120 hpi, the differences became apparent and statistically significant with SP-EGFP-PDCB1 unable to spread efficiently between cells (Fig. 3a). Thus, the data in Fig. 3a indicate the ability of PDLP5 to traffic between plant cells. PDCB1 either does not possess the capacity for cell-to-cell movement, or this capacity is very limited. Finally, we compared the movement of PDLP5 to that of the classical and efficient PD-moving proteins, MPs of tobamoviruses[24,30,31]; specifically, we utilized TVCV MP[32]. Figure 3b shows that TVCV MP indeed exhibited extensive cell-to-cell movement, with its frequency reaching ca. 80% of all initially expressing cells, and the movement of PDLP5 was lower, with ca. 50% frequency. In contrast, we detected significantly lower levels of PDCB1 movement, ca. 30% (Fig. 3b), at least some of which potentially represent protein diffusion through PD known to occur with other proteins[33,34].

PDLP1 and PDLP2 do not move from cell to cell efficiently

We then examined whether cell-to-cell movement is a general property of PDLPs. From the eight known members of this protein family[3], we selected two proteins, PDLP1 and PDLP2, which share 24.92% and 24.76% identity in amino acid sequence compared to PDLP5, respectively, tagged them with EGFP, and assayed potential movement. Figure 3c shows the two-cell clusters of SP-EGFP-PDCB1, PDLP1-EGFP, and PDLP2-EGFP, respectively. However, both PDLP1-EGFP and PDLP2-EGFP exhibited only low levels of the spread between cells, comparable to that of SP-EGFP-PDCB1, with no statistically significant differences between them whereas, in the

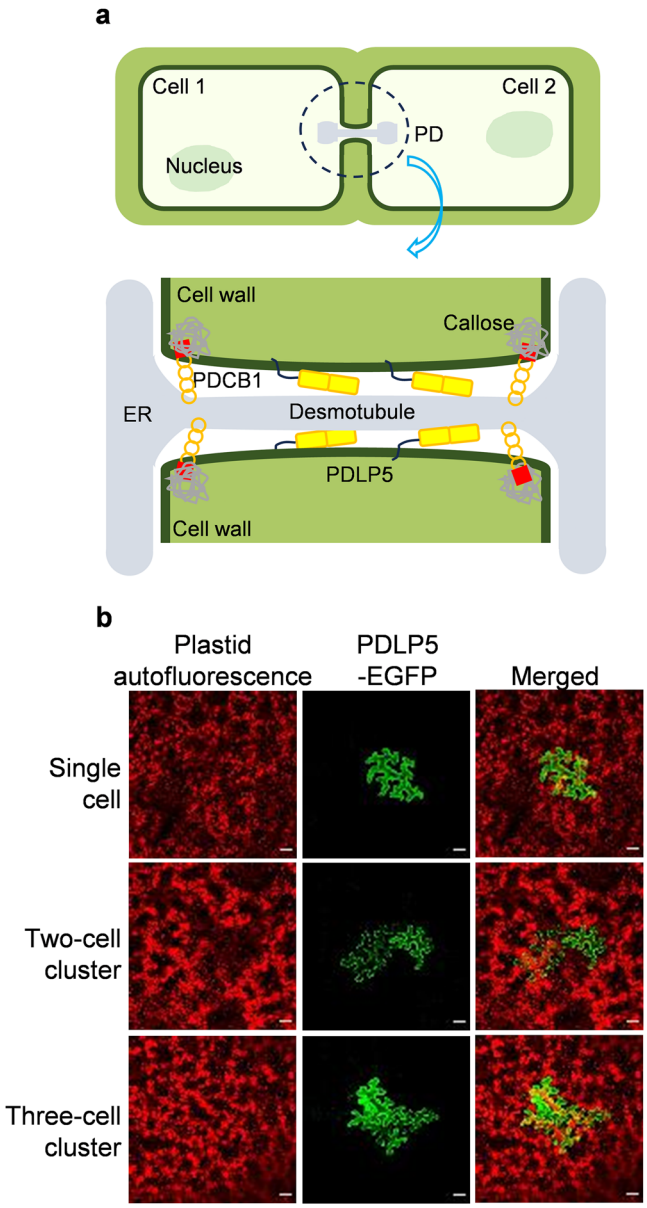

Fig. 1 | Plasmodesmata (PD) and PDLP5 cell-to-cell movement. a A schematic representation of PD and its relevant components, i.e., PDLP5[4,19] and PDCB1[28,29], examined in this study. The ER-derived trans-PD desmotubule and callose deposits at the neck regions of PD are indicated. **b** Visualization of the cell-to-cell movement of PDLP5-EGFP. Images were recorded at 72 hpi and are single confocal sections representative of multiple independent experiments ($n = 3$ biological replicates, containing 20 images from 4 plants in each of them). Single-cell or multi-cell clusters represent the absence or presence of cell-to-cell movement, respectively. Scale bars = 50 µm.

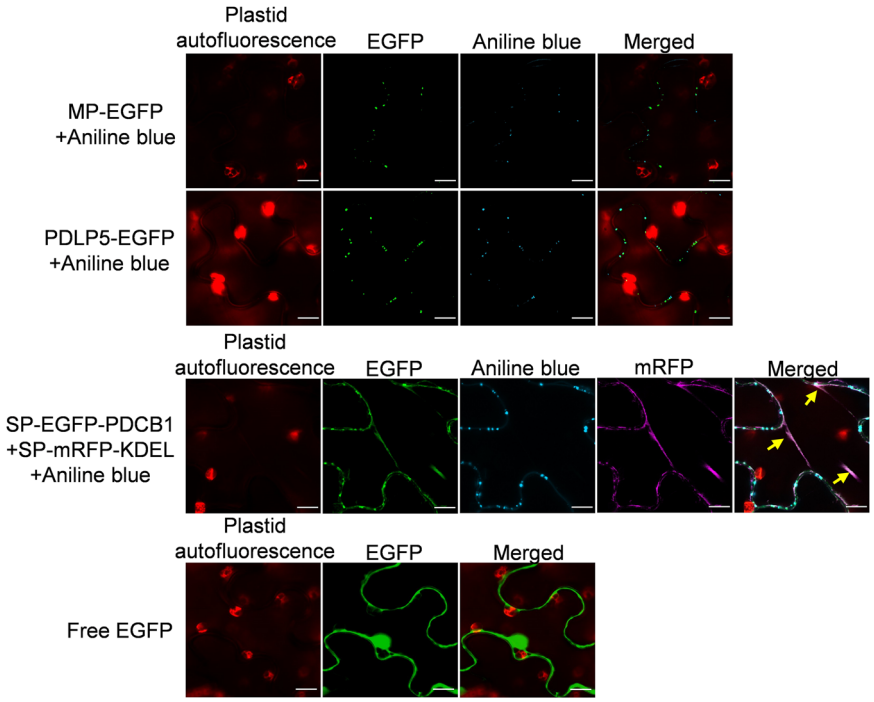

Fig. 2 | PD accumulation of transiently expressed PDLP5. Images were recorded at 2 dpi and are single confocal sections representative of 40 images from different plants. The EGFP signal is in green, the aniline blue signal is in blue, the mRFP signal is in pink, and the plastid autofluorescence is in red. Yellow arrows show the colocalization of PDCB1 with the ER. Scale bars = 10 µm.

positive control, PDLP5-EGFP moved more efficiently and with statistical significance (Fig. 3d). Thus, the cell-to-cell movement ability of PDLP5 does not represent a common function of PDLP proteins.

The transmembrane domain of PDLP5 participates in PDLP5 movement

The regulation of PD permeability represents the main biological function of PDLP5, and this activity requires the Ax_3G motif located in the TMD of the protein[19]. Thus, it was interesting to explore whether the Ax_3G motif or TMD also participates in the PDLP5 cell-to-cell movement. Figure 4a shows the predicted structural model obtained from the AlphaFold Protein Structure Database (https://alphafold.ebi.ac.uk/) for PDLP5 with the TMD sequence highlighted. We constructed three PDLP5 mutants in this sequence[19,35]: $PDLP5^{VV}$ in which alanine 266 and glycine 270 of the Ax_3G motif were substituted with valine, and $PDLP5^{ACR4}$ and $PDLP5^{BAK1}$ in which the native TMD sequence from leucine 265 to glycine 286—as predicted by the Biosequence analysis using profile hidden Markov Models (https://www.ebi.ac.uk/Tools/hmmer/search/hmmscan)—was substituted with the TMD domains from the receptor-like protein kinases (RLPKs) Arabidopsis CRINKLY 4 (ACR4) or BARELY ANY MERISTEM 1 (BAK1), respectively (Fig. 4a). We then tested whether these mutations interfered with the optimal movement capacity of PDLP5 which was higher in a statistically significant fashion than that of the PDCB1 basal movement control (Fig. 4b). Figure 4b shows that each of the mutants exhibited reduced movement capacity which remained slightly higher than that of PDCB1 but without statistical significance. These observations implicate the native TMD sequence of PDLP5 in the ability of this protein to move through PD.

Discussion

PD protein components, including the PDLP protein family, have received significant attention mainly due to their potential roles in the regulation and facilitation of molecular traffic through the PD channels. However, the possible ability of the PD proteins themselves to traverse PD and move to the neighboring cells has not been adequately addressed. We started filling this knowledge gap by investigating the cell-to-cell movement capacity of PDLP5, a functionally important PD protein that restricts PD permeability and promotes innate immunity. Our studies of the intercellular distribution patterns of PDLP5 following its initial transient expression in plant leaves revealed that PDLP5 is not strictly cell-autonomous in 40–60% of the expressing cells. This movement efficiency was lower but still comparable to the 80% movement observed with the paradigm of PD-moving proteins, the tobamoviral MP. In contrast, other tested PD proteins, PDCB1, PDLP1, and PDLP2, showed much weaker ability, i.e., 20–30%, to spread between cells. This study examined the idea that PDLP5, a resident PD protein, may move between cells and did not aim to elucidate the mechanism(s) of this movement; yet we speculate that it could occur via lateral diffusion of a fraction of PDLP5 in the plasma membrane. Interestingly, earlier data suggested that PDLP5 is largely immobile at PD, with only 5% of the protein showing lateral movement[19] and it was considered a cell-autonomous protein[36]; however, initially, this immobility was determined using fluorescence recovery after photobleaching (FRAP) after 100 s[19] and subsequently, using imaging of the PDLP5-CFP accumulation patterns[36], which also were analyzed for up to 60 h whereas our observations suggest that significant movement of PDLP5-EGFP is detected at 72 h, the prolonged period over which the small mobile fraction of PDLP5 moved between cells. Alternatively, following the expression of PDLP5 in the cell cytoplasm, some of the protein may first move through PD and only then integrate into the plasma membrane in the PD of the adjacent cell. On the other hand, the possibility of movement of misfolded PDLP5-EGFP is unlikely because its molecules exhibited their native pattern of PD localization following their transit to another cell (see Fig. 1b).

The ability of PDLP5 to move through PD involves its TMD as mutations in this sequence reduced movement; furthermore, the optimal movement required the native TMD of PDLP5 because its replacement with "heterologous" TMDs from one of the two RLK proteins also reduced movement. This contrasts with the PD localization of PDLP5 in individual plant cells, which did not require native TMD and was not affected by mutations in its Ax3G motif[19]. The involvement of TMD in PDLP5 movement through the PD channel suggests that this process is facilitated by this channel's membranous components, such as desmotubule. Because science is iterative, scientific inquiry usually leads to new questions. The main question raised by the observation of the PDLP5 capacity for cell-to-cell movement is whether this capacity is involved in the known biological functions of PDLP5, i.e., negative regulation of PD permeability and facilitation of innate immunity, or whether PDLP5 might fulfill another, yet unknown, function in the plant intercellular communication.

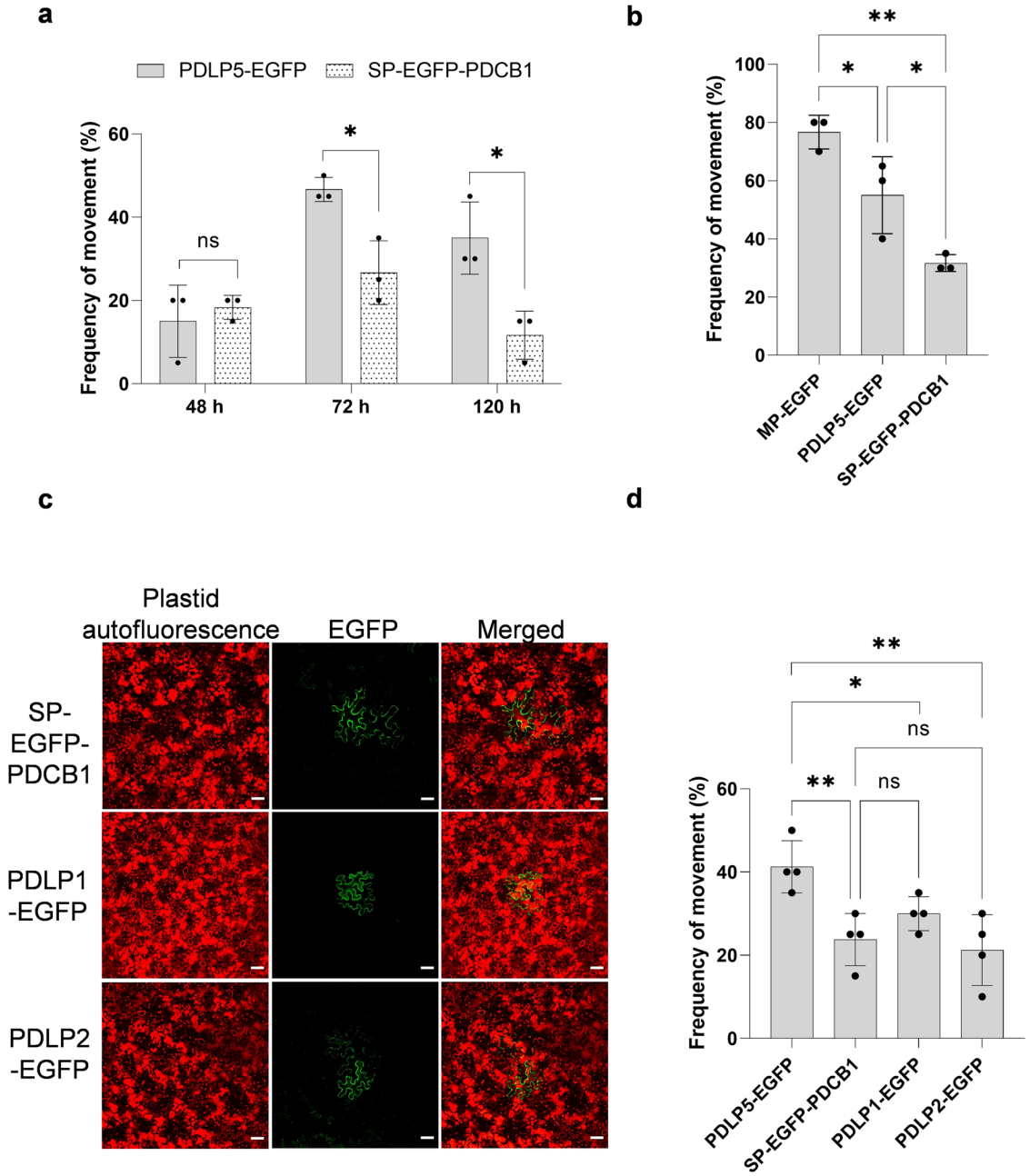

Fig. 3 | Quantification of cell-to-cell movement of PDLP5, PDCB1, PDLP1, and PDLP2. a Time course of PDLP5-EGFP (gray bars) and SP-EGFP-PDCB1 movement (dotted bars). **b** Movement of MP-EGFP, PDLP5-EGFP, and SP-EGFP-PDCB1. **c** Visualization of the two-cell clusters of SP-EGFP-PDCB1, PDLP1-EGFP, and PDLP2-EGFP. Images were recorded at 72 hpi and are single confocal sections representative of multiple independent experiments. Scale bars = 50 µm. **d** Movement of PDLP5-EGFP, SP-EGFP-PDCB1, PDLP1-EGFP, and PDLP2-EGFP. The movement was scored at 72 hpi. Error bars represent the standard deviation of the means from multiple experiments. The individual data points are indicated as the mean value for each independent experiment ($n = 3$–4 biological replicates, containing 20 images from 3 or 4 plants in each of them). Differences between mean values assessed by the one-way ANOVA with Tukey's multiple comparisons test (**b** and PDLP1/PDLP2/PDLP5 vs. PDCB1 in **d**) and the Student's *t*-test (panel **a** and PDLP5 vs. PDLP1/PDLP2 in **d**) are statistically significant for the *P*-values $^{*}P < 0.05$, and $^{**}P < 0.01$; $P \geq 0.05$ is not statistically significant (ns).

Methods

Plant material and bacterial strains

Nicotiana benthamiana plants were grown in controlled environment growth chambers at 23 °C under 16-h-light conditions for transient expression assays. *Escherichia coli* strain DH10B was cultured at 37 °C in Lysogeny Broth (LB) broth or LB agar. *Agrobacterium tumefaciens* strain EHA105 was cultured at 28 °C in LB broth or LB agar for transient expression assays. The growth media were supplemented with antibiotics at the following concentrations: gentamicin (10 µg/ml), spectinomycin (50 µg/ml), and rifampicin (25 µg/ml). All strains and their derivatives are listed in Supplementary Table 1.

Plasmid construction

Different coding sequences were amplified by PCR or overlap PCR using Q5® High-Fidelity DNA Polymerase (#M0491S, NEB) and cloned into pDONR207 (#12213013, Invitrogen) by the BP reaction using Gateway BP Clonase II (#11789020, Invitrogen). Each of the target genes, except *PDCB1*, in the resulting entry plasmid was then transferred into the destination vector pPZP-RCS2A-nptII-DEST-EGFP-N1 (obtained from the late Dr. Michael Goodin, University of Kentucky) by the LR reaction using Gateway LR Clonase II (#11791020, Invitrogen), resulting in expression constructs with the EGFP fused to the C-terminus of PDLP1, PDLP2, or PDLP5 and PDLP5 mutants. The *PDCB1* sequence was transferred to pPZP-RCS2A-

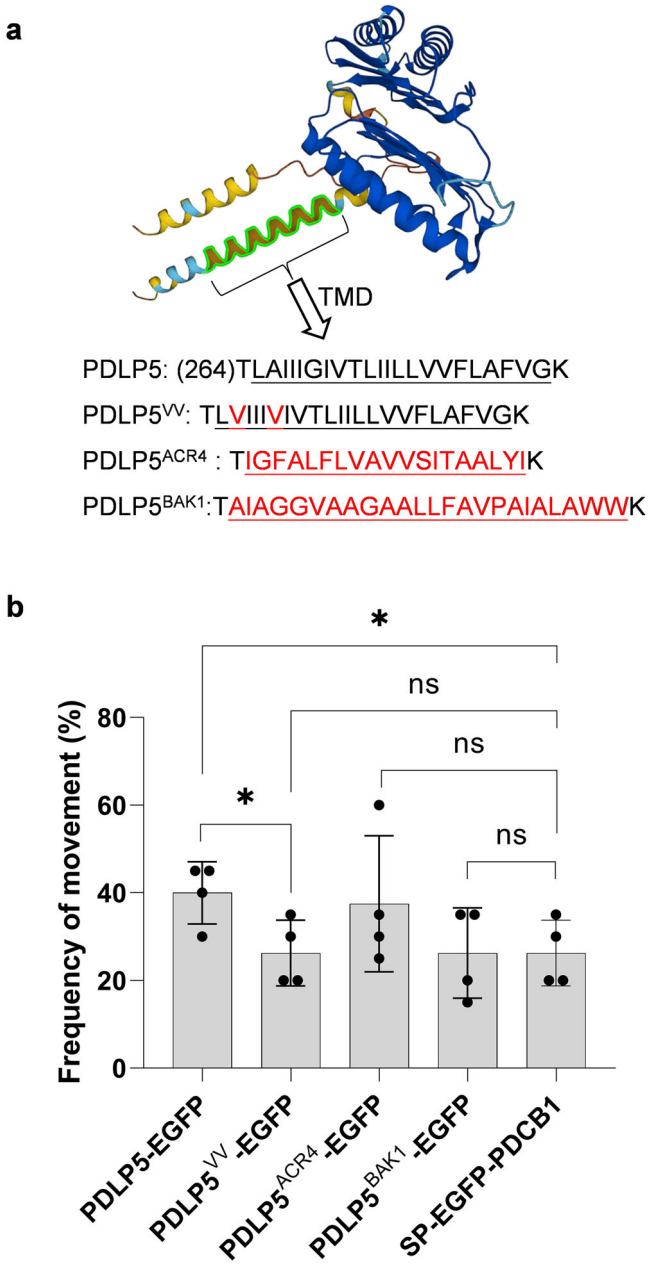

Fig. 4 | Quantification of cell-to-cell movement of PDLP5 mutants. a AlphaFold-based prediction of the PDLP5 structure. TMD is highlighted in green, the amino acid sequences of TMD and its mutant derivatives are indicated with the mutated residues in red font, and the entire length of TMD is underlined. **b** Movement of PDLP5-EGFP and its mutant derivatives. Error bars represent the standard deviation of the means from multiple experiments. The individual data points are indicated as the mean for an independent experiment ($n = 4$ biological replicates, containing 20 images from 4 plants in each of them). Differences between mean values assessed by the Student's *t*-test are statistically significant for the *P*-values $^*P < 0.05$; ns not significant.

nptII-DEST by the LR reaction using Gateway LR Clonase II, resulting in an expression construct with EGFP positioned immediately downstream the signal peptide (SP) of PDCB1 and leaving the C-terminus of PDCB1 free as described[28,29]. pPZP-RCS2A-nptII-DEST (also obtained from Dr. Goodin) was generated by inserting the PIPspI fragment of pSAT6A-DEST (GenBank accession number EF212310.1)[37] into the PIPspI-digested pRCS2-ocs-nptII binary vector (GenBank accession number DQ005456)[38] The ER-targeted SP-mRFP-KDEL protein was expressed from pMDC32-SP-mRFP-KDEL generated from pImpactVector1.3-mRFP (Plant Research International, Wageningen, The Netherlands)[39]. All constructs were verified by PCR and sequencing. All plasmids and primers are listed in Supplementary Table 1.

Agroinfiltration and confocal imaging

For the cell-to-cell movement assay, plasmids encoding the tested proteins tagged with EGFP at their C-termini were transformed into *Agrobacterium tumefaciens* strain EHA105. One milliliter overnight culture of *A. tumefaciens* EHA105 harboring the tested constructs was transferred into 4 ml fresh LB and grown for an hour. The bacterial suspensions were washed once with 5 ml of 10 mM $MgCl_2$ to remove the growth medium and then centrifuged and resuspended with the infiltration buffer containing 10 mM $MgCl_2$ and 10 mM 2-(N-morpholino)-ethanesulfonic acid (MES) (pH 5.6). The bacterial cultures were then diluted to $OD_{600\ nm} = 5 \times 10^{-4}$ with the infiltration buffer, incubated for 3 h at room temperature with soft shaking, and infiltrated into the adaxial surface of the leaves of 4 to 5-week-old *N. benthamiana* plants with a needleless syringe. Three days, unless indicated otherwise, after the infiltration, the infiltrated areas were visualized using a laser scanning confocal microscope (LSM 900, Zeiss) with a ×10 objective lens and GFP filters. Twenty images were acquired from four different leaves of four different plants in each experiment, and there were at least three independent experiments. Single cells, indicating no cell-to-cell movement, and clusters of two or three cells, indicating cell-to-cell movement, were scored. The movement frequency was calculated using the formula: frequency of movement = number of multi-cell clusters / 20 × 100%. For the protein subcellular localization assay, *A. tumefaciens* strain EHA105 cells were induced and infiltrated *N. benthamiana* leaves under the same conditions. For the PDCB1 localization assay, the EHA105 cells carrying the SP-mRFP-KDEL expression construct were co-infiltrated with the EHA105 cells carrying the SP-EGFP-PDCB1 expression construct. Two days later, aniline blue staining was proceeded as Huang et al. described[40], briefly, infiltrated area of approximately 0.5 cm × 0.5 cm was excised and submerged in 200 µl of 1% aniline blue (in 50 mM potassium phosphate buffer, pH 8.0) on the microscope slide, and then cover it with a cover glass (22 mm × 50 mm). Place the microscope slides with the samples in a desiccator attached to a vacuum pump and evacuate for 2 min (<0.8 Pa), followed by a slow release of the pressure and incubation in the dark for 30 min at room temperature. Excitation wavelengths for the detection of CFP and GFP signals are 405 nm and 488 nm, respectively, and the emission filters for detection were 400–602 nm with the pinhole 1 AU and the Master Gain set as 769 V.

Statistical analysis

All the experiments in this manuscript were repeated at least three times, and the one-way ANOVA with Tukey's multiple comparisons test or the Student's *t*-test was used to determine the P-values between the different samples with GraphPad Prism 9.0.0.

Data availability

Data is provided within the manuscript or supplementary information files.

Received: 17 June 2024; Accepted: 1 April 2025;
Published online: 01 July 2025

References

1. Bayer, E. M. & Benitez-Alfonso, Y. Plasmodesmata: channels under pressure. *Annu. Rev. Plant Biol.* **75**, 21.1–21.27 (2024).
2. Wang, Y. et al. Plasmodesmata mediate cell-to-cell transport of brassinosteroid hormones. *Nat. Chem. Biol.* **19**, 1331–1341 (2023).
3. Thomas, C. L., Bayer, E. M., Ritzenthaler, C., Fernandez-Calvino, L. & Maule, A. J. Specific targeting of a plasmodesmal protein affecting cell-to-cell communication. *PLoS. Biol.* **6**, e7 (2008).
4. Lee, J. et al. A plasmodesmata-localized protein mediates crosstalk between cell-to-cell communication and innate immunity in *Arabidopsis*. *Plant Cell* **23**, 3353–3373 (2011).
5. Benitez-Alfonso, Y., Faulkner, C., Ritzenthaler, C. & Maule, A. J. Plasmodesmata gateways to local and systemic virus infection. *Mol. Plant Microbe Interact.* **11**, 1403–1412 (2010).

6. Maule, A. J. Plasmodesmata: structure, function and biogenesis. *Curr. Opin. Plant Biol.* **11**, 680–686 (2008).
7. Kraner, M. E., Müller, C. & Sonnewald, U. Comparative proteomic profiling of the choline transporter-like1 (CHER1) mutant provides insights into plasmodesmata composition of fully developed *Arabidopsis thaliana* leaves. *Plant J.* **92**, 696–709 (2017).
8. Johnston, M. G. et al. Comparative phyloproteomics identifies conserved plasmodesmal proteins. *J. Exp. Bot.* **74**, 1821–1835 (2023).
9. Kirk, P., Amsbury, S., German, L., Gaudioso-Pedraza, R. & Benitez-Alfonso, Y. A comparative meta-proteomic pipeline for the identification of plasmodesmata proteins and regulatory conditions in diverse plant species. *BMC Biol.* **20**, 128 (2022).
10. Fernandez-Calvino, L. et al. *Arabidopsis* plasmodesmal proteome. *PLoS One* **6**, e18880 (2011).
11. Radford, J. E., Vesk, M. & Overall, R. L. Callose deposition at plasmodesmata. *Protoplasma* **201**, 30–37 (1998).
12. Levy, A., Erlanger, M., Rosenthal, M. & Epel, B. L. A plasmodesmata-associated β-1,3-glucanase in *Arabidopsis*. *Plant J.* **49**, 669–682 (2007).
13. Kankanala, P., Czymmek, K. & Valent, B. Roles for rice membrane dynamics and plasmodesmata during biotrophic invasion by the blast fungus. *Plant Cell* **19**, 706–724 (2007).
14. Aung, K. et al. Pathogenic bacteria target plant plasmodesmata to colonize and invade surrounding tissues. *Plant Cell* **32**, 595–611 (2020).
15. Ueki, S. & Citovsky, V. To gate, or not to gate: regulatory mechanisms for intercellular protein transport and virus movement in plants. *Mol. Plant* **4**, 782–793 (2011).
16. Amari, K. et al. A family of plasmodesmal proteins with receptor-like properties for plant viral movement proteins. *PLoS Pathog.* **6**, e1001119 (2010).
17. Liu, N. J. et al. Phytosphinganine affects plasmodesmata permeability via facilitating PDLP5-stimulated callose accumulation in *Arabidopsis*. *Mol. Plant* **13**, 128–143 (2020).
18. Wang, X. et al. Salicylic acid regulates plasmodesmata closure during innate immune responses in *Arabidopsis*. *Plant Cell* **25**, 2315–2329 (2013).
19. Wang, X., Robles Luna, G., Arighi, C. N. & Lee, J. An evolutionarily conserved motif is required for plasmodesmata-located protein 5 to regulate cell-to-cell movement. *Commun. Biol.* **3**, 291 (2020).
20. Vaattovaara, A. et al. Mechanistic insights into the evolution of DUF26-containing proteins in land plants. *Commun. Biol.* **2**, 56 (2019).
21. Lim, G. et al. Plasmodesmata localizing proteins regulate transport and signaling during systemic acquired immunity in plants. *Cell Host Microbe* **19**, 541–549 (2016).
22. Caillaud, M. C. et al. The plasmodesmal protein PDLP1 localises to haustoria-associated membranes during downy mildew infection and regulates callose deposition. *PLoS Pathog.* **10**, e1004496 (2014).
23. Yuan, C., Lazarowitz, S. G. & Citovsky, V. Identification of a functional plasmodesmal localization signal in a plant viral cell-to-cell-movement protein. *mBio* **7**, e02052–15 (2016).
24. Tran, P. T., Vo, P. M. & Citovsky, V. Gain-of-function mutant of movement protein allows systemic transport of a defective tobacco mosaic virus. *iScience* **25**, 105486 (2022).
25. Roberts, I. M. et al. Dynamic changes in the frequency and architecture of plasmodesmata during the sink-source transition in tobacco leaves. *Protoplasma* **218**, 31–44 (2001).
26. Ueki, S., Lacroix, B., Krichevsky, A., Lazarowitz, S. G. & Citovsky, V. Functional transient genetic transformation of *Arabidopsis* leaves by biolistic bombardment. *Nat. Protoc.* **4**, 71–77 (2009).
27. Yuan, C., Lazarowitz, S. G. & Citovsky, V. The plasmodesmal localization signal of TMV MP is recognized by plant synaptotagmin SYTA. *mBio* **9**, e01314–e01318 (2018).
28. Simpson, C., Thomas, C., Findlay, K., Bayer, E. & Maule, A. J. An *Arabidopsis* GPI-anchor plasmodesmal neck protein with callose binding activity and potential to regulate cell-to-cell trafficking. *Plant Cell* **21**, 581–594 (2009).
29. Zavaliev, R., Dong, X. & Epel, B. L. Glycosylphosphatidylinositol (GPI) modification serves as a primary plasmodesmal targeting signal. *Plant Physiol.* **172**, 1061–1073 (2016).
30. Schoelz, J. E., Harries, P. A. & Nelson, R. S. Intracellular transport of plant viruses: finding the door out of the cell. *Mol. Plant* **4**, 813–831 (2011).
31. Tagami, Y. & Watanabe, Y. Effects of brefeldin A on the localization of *Tobamovirus* movement protein and cell-to-cell movement of the virus. *Virology* **361**, 133–140 (2007).
32. Levy, A., Zheng, J. Y. & Lazarowitz, S. G. The tobamovirus turnip vein clearing virus 30-kilodalton movement protein localizes to novel nuclear filaments to enhance virus infection. *J. Virol.* **87**, 6428–6440 (2013).
33. Crawford, K. M. & Zambryski, P. C. Subcellular localization determines the availability of non-targeted proteins to plasmodesmatal transport. *Curr. Biol.* **10**, 1032–1040 (2000).
34. Crawford, K. M. & Zambryski, P. C. Non-targeted and targeted protein movement through plasmodesmata in leaves in different developmental and physiological states. *Plant Physiol.* **125**, 1802–1812 (2001).
35. Stahl, Y. et al. Moderation of *Arabidopsis* root stemness by CLAVATA1 and ARABIDOPSIS CRINKLY4 receptor kinase complexes. *Curr. Biol.* **23**, 362–371 (2013).
36. Tran, P. & Citovsky, V. Receptor-like kinase BAM1 facilitates early movement of the tobacco mosaic virus. *Commun. Biol.* **4**, 511 (2021).
37. Chakrabarty, R. et al. pSITE vectors for stable integration or transient expression of autofluorescent protein fusions in plants: probing *Nicotiana benthamiana*-virus interactions. *Mol. Plant Microbe Interact.* **20**, 740–750 (2007).
38. Chung, S., Frankman, E. L. & Tzfira, T. A versatile vector system for multiple gene expression in plants. *Trends Plant Sci.* **10**, 357–361 (2005).
39. Mirauti, A., Tran, P. & Citovsky, V. Restriction-ligation-independent production of a TVCV infectious clone and a TVCV-based gene expression vector. *Heliyon* **9**, e19855 (2023).
40. Huang, C. et al. dsRNA-induced immunity targets plasmodesmata and is suppressed by viral movement proteins. *Plant Cell* **35**, 3845–3869 (2023).

Acknowledgements

The work in the V.C. laboratory was supported by grants from NIH (R35GM144059), NSF (MCB 1913165), and BARD (IS-5276-20) to V.C. The funders had no role in study design, data collection and interpretation, or the decision to publish.

Author contributions

V.C. conceived the project. Y.K. performed research; Y.K. and V.C. wrote the manuscript.

Competing interests

The authors declare no competing interests.

Additional information

Supplementary information The online version contains supplementary material available at https://doi.org/10.1038/s44383-025-00001-9.

Correspondence and requests for materials should be addressed to Yumin Kan.